Near-infrared light-emitting ambipolar organic field-effect transistors

Smits, Edsger C. P.; Setayesh, Sepas; Anthopoulos, Thomas D.; Buechel, Michael; Nijssen, Wim; Coehoorn, Reinder; Blom, Paul W. M.; de Boer, Bert; de Leeuw, Dago M.

Published in:
Advanced materials

DOI:
10.1002/adma.200600999

Publication date:
2007

ADVANCED MATERIALS

DOI: 10.1002/adma.200600999

Near-Infrared Light-Emitting Ambipolar Organic Field-Effect Transistors**

By *Edsger C. P. Smits*, *Sepas Setayesh*, *Thomas D. Anthopoulos*, *Michael Buechel*, *Wim Nijssen*, *Reinder Coehoorn*, *Paul W. M. Blom*, *Bert de Boer*, and *Dago M. de Leeuw**

Recent years have seen tremendous advances in the area of organic-based optoelectronic devices and several applications previously envisioned are now reaching the stage of commercial exploitation.[1] Organic field-effect transistors (OFETs) are among these devices and can be arguably viewed as a possible alternative to their inorganic counterparts in a range of low-cost high-volume applications.[2] Traditionally, OFETs have been used as pixel switches in active matrix displays and as the building blocks of integrated circuits where mechanical flexibility and low-cost fabrication are two prerequisites.[1] Recently, novel bifunctional OFETs have also made their debut where, in addition to their classical current-modulating function, light-emission from within the electroactive channel has been reported.[3] Such electro-optical transistors are interesting for two reasons: First, the ability of combining optoelectronic functionalities in a single device will increase the number of potential applications, like integrated circuits for signal-processing that involve both optical and electrical signals. Secondly, it will provide an ideal experimental platform for the study of various fundamental physical processes (optical and electronic) characteristic in organic semiconductors.

[*] Dr. D. M. de Leeuw, E. C. P. Smits, Dr. S. Setayesh, Dr. M. Buechel, W. Nijssen, Prof. R. Coehoorn
Philips Research Laboratories
High Tech Campus 4 (WAG 11)
5656 AE Eindhoven (The Netherlands)
E-mail: dago.de.leeuw@philips.com
E. C. P. Smits, Prof. P. W. M. Blom, Dr. B. de Boer
Molecular Electronics, Material Science Centreplus
University of Groningen
Nijenborgh 4, 9747 AG Groningen (The Netherlands)
E. C. P. Smits
Dutch Polymer Institute
Nijenborgh 4, 9747 AG Groningen (The Netherlands)
Dr. T. D. Anthopoulos
Department of Physics, Blackett Laboratory
Imperial College London
London SW7 2BW (UK)

[**] The work of E.C.P.S. forms part of the research program of the Dutch Polymer Institute (DPI) project No: 516. T.D.A. is grateful to EC (HPRN-CT-2002-00327) and EPSRC for financial support. T.D.A. is an EPSRC Advanced Research Fellow. D.M.D.L. and R.C. gratefully acknowledge the support of the EU projects NAIMO (NMP4-CT-2004-500355) and RADSAS (NMP3-CT-2004-001561). We are grateful to Piet Rommers, Inge Vorstenbosch, and Otto Muskens for their help with performing the CV, PL, and EL measurements and to Eduard Meijer for his useful discussions.

To date several types of light-emitting OFETs (LEOFETs) have been demonstrated. The majority of these devices are "unipolar" in nature (capable of transporting a single charge-carrier type, i.e., holes or electrons). As a consequence light emission occurs only at the interface between the semiconductor and the minority-carrier injecting electrode.[3–8] Only recently light emission from within the transistor channel was demonstrated in ambipolar OFETs (i.e., capable of transporting both holes and electrons).[9–14] In an ambipolar LEOFET when the gate is biased in between the source and drain potentials, holes and electrons are injected simultaneously at the opposite ends of the channel. At the point where the local potential within the channel equals the gate potential a pn-junction is formed at which opposite carriers can recombine to form excitons. When these excitons undergo radiative decay, the device emits light. The position of the so-called "recombination zone" can in principle be tuned along the channel by simply adjusting the gate potential, V_g, and drain potential, V_d. This has been indeed demonstrated in the recent works by Zaumseil et al.[12] and Swensen et al.[13] In both studies, LEOFETs were fabricated using dissimilar source and drain contact materials to facilitate injection and transport of both holes and electrons. The use of dissimilar contacts in combination with suitable gate dielectrics[15] has been the most suitable method shown so far for fabricating truly ambipolar LEOFETs.

In this paper, we demonstrate an alternative approach towards ambipolar LEOFETs based on a solution-processable small-bandgap squarylium dye. Simultaneous injection of holes and electrons can be obtained leading to ambipolar transistor operation because of the low energy gap of the dye and its favorable position relative to the Fermi level of both gold source and drain electrodes. Under appropriate bias conditions holes and electrons recombine within the channel and the transistor emits light in the near-infrared region of the electromagnetic spectrum. By invoking an ambipolar-transistor model we are able to estimate the position of the recombination zone, at all biasing regimes. Based on these calculations, the measured change in quantum efficiency as a function of recombination position within the channel can be explained. The quantum efficiency of the device is found to depend only weakly on the position of the recombination zone along the channel, as long as the recombination zone is not close to the source or drain contact.

The 2,4-di-3-guaiazulenyl-1,3-dihydroxycyclobutenediylium-dixydroxide-bis inner salt (SQ1) employed here was pur-

chased from Aldrich Chem. Co. and used directly for device fabrication without further purification. The molecular structure of SQ1 is shown in the inset of Figure 1. The material was found to be highly soluble in a variety of common organic solvents. The UV-vis absorption spectrum in the solid-state

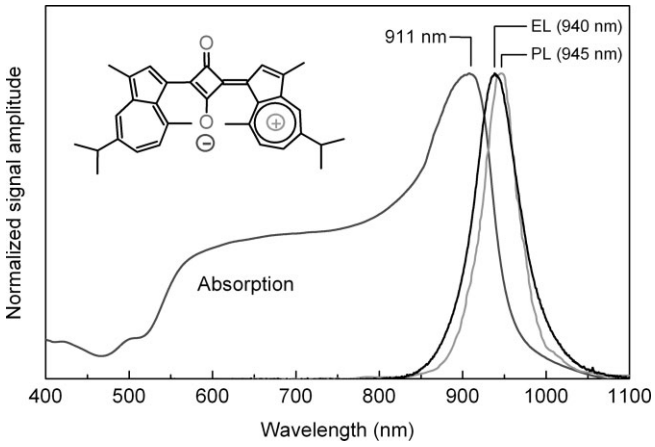

Figure 1. UV-vis absorption, photoluminescence (PL), and electroluminescence (EL) spectra for an SQ1 film. The inset shows the molecular structure of SQ1.

(thin film) is shown in Figure 1. A single peak at approximately 911 nm is observed. From the absorption onset of the spectrum, the energy gap between the highest molecular orbital (HOMO) and lowest unoccupied molecular orbital (LUMO) is calculated to be 1–1.2 eV. In the solid state, the HOMO–LUMO gap was determined using an electrochemical technique with the dye deposited on a glassy carbon electrode employing dichloromethane as the solvent. From the onset of the redox peaks a bandgap of ca. 1.2 eV was determined with HOMO and LUMO levels respectively at –5.0 eV and –3.8 eV with respect to the vacuum level. Photoluminescence (PL) measurements were also performed on annealed films of SQ1 using a 633 nm excitation wavelength from a diode laser. The obtained spectrum is shown in Figure 1 where a narrow emission peak can be observed at 945 nm. Radiative recombination was confirmed by using electroluminescence (EL) measurements. The EL spectrum obtained for an ITO/SQ1/Ba(Al) diode was similar to the PL spectrum, as shown in Figure 1.

Bottom-contact field-effect transistors were fabricated by solution-processing SQ1 on the top of prepatterned substrates.[16] Details of the fabrication process are given in the Experimental section. Figure 2a (symbols) shows the ambipolar transfer characteristics of a SQ1-based transistor at different biasing regimes. The solid lines represent the simulated curves using the ambipolar transport model discussed later.[16] The maximum hole and electron mobilities derived from the transfer curves of Figure 2a are approximately equal and in the order of 10^{-4} $cm^2 V^- s^{-1}$. We note, however, that mobility values were strongly dependent on the film morphology because of the crystallization occurring upon annealing, which

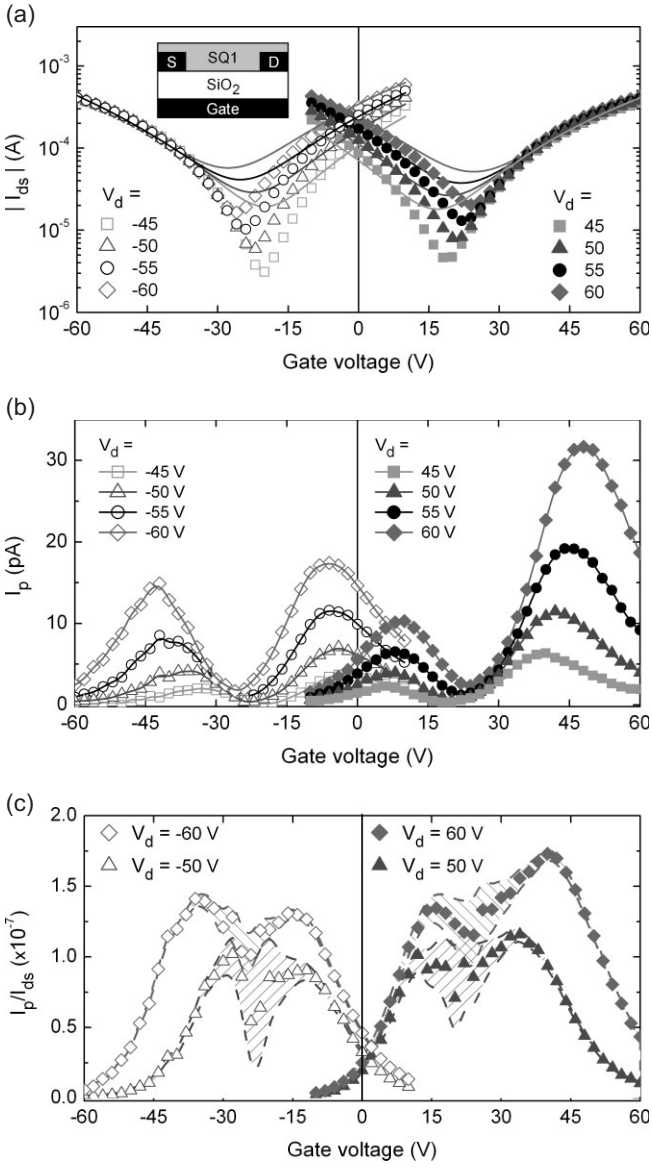

Figure 2. a) Transfer characteristics of an ambipolar transistor (channel length $L = 2.5$ μm, and width $W = 50$ cm) based on SQ1 at different biasing regimes. Symbols represent the experimental results and solid lines the theoretical fits using the ambipolar model as described by Smits et al. [16] The fitting parameters employed are summarized in the text. The inset shows the schematic of the bottom-contact transistor architecture employed. b) The light intensity measured with a photodiode (I_p) positioned above the transistor as a function of drain and gate biases. c) The ratio of the measured photodiode current over drain current (I_p/I_{ds}) versus gate bias (V_g) at different drain voltages. The shadowed area represents the estimated error caused by the photodiodes dark current.

led to a significant parameter spread between samples. For our best transistors hole mobilities as high as 1×10^{-3} $cm^2 V^- s^{-1}$ were measured.

Under appropriate bias conditions we observed infrared-light emission from within the electroactive transistor channel. Figure 2b shows the photodiode current (I_p) as a function of positive and negative V_g and V_d voltages. For each biasing

ADVANCED MATERIALS

regime the photodiode current showed two maxima, the position of which depended on the V_d voltage. We observed that when the source–drain current is at a minimum, which was the case when $V_g - V_t \approx V_d/2$ for similar hole and electron mobilities, the photodiode current was also at a minimum. This was, however, the position where the recombination was calculated to be located in the middle of the channel. As I_p is proportional to the number of emitted photons from within the channel of the ambipolar OFET, and the source–drain current (I_{ds}) is expected to be proportional to the number of injected carriers (holes and electrons), we plotted the ratio of I_p/I_{ds} ($\propto$ external quantum efficiency) versus V_g at different V_d voltages. These results are displayed in Figure 2c. The shadowed areas represent the error margins for each measured point, which were introduced by the dark current in the photodiode (0.1–0.5 pA). This dark current, although very low, was comparable to I_{ds} for V_g, where I_{ds} was at a minimum (see Fig. 2a) and responsible for the I_p/I_{ds} uncertainty in this V_g region. Overall, a slight increase in I_p/I_{ds} with increasing current was observed, the origin of which is not understood at present. It is evident from this figure that the trace resembles a single broad peak/plateau with a small substructure (at each biasing regime). These are in agreement with results previously published.[12] This broad peak emission occurs when the device is operated in a pn-junction regime ($|V_d| > |V_g - V_t| > 0$, where V_t is the threshold voltage).

The reduction of emitted light at higher and lower V_g has also been observed previously for LEOFETs driven in constant-current mode. Zaumseil et al.[12] have argued that there are two possible mechanisms responsible for this observation: one is the metal-induced EL quenching occurring near the metal electrodes, and the second is the direct transport of electrons and/or holes to the metal electrode without recombining. For the latter mechanism to occur, the recombination zone has to be in very close proximity to the metal electrode, which would mean that the transistor would start to operate in unipolar mode. To elucidate the origin of this effect in our devices we employed a microscopic transport model developed recently for ambipolar organic transistors.[16] This model is based on the variable-range hopping theory in an exponential density of states (DOS)[17] and has been shown to give a fair description of OFETs based on disordered semiconductors.[18] We assume that in the ambipolar transistor complete charge recombination occurs in a planar zone perpendicular to the channel, with a width that is much smaller than the source–drain distance. Under these circumstances we may approximate the device to consist of two spatially separated transistors, an n-type and a p-type, connected in series. The length of each transistor (L_e for electrons and L_h for holes with $L = L_e + L_h$) depends on the drain and gate voltages. This implies that at each electrode the current is carried only by one type of charge carrier, hence the current in the electron channel can be written as

$$I_{ds,e}(x < x_0) = \frac{W}{x_0}\left(\gamma_e \frac{T}{2T_{0,e}} \frac{T}{2T_{0,e} - T}\left(V_g - V_t\right)^{\frac{2T_{0,e}}{T}}\right) \quad (1)$$

with

$$\gamma_e = \frac{\sigma_{0,e}}{q}\left(\frac{\left(\frac{T_{0,e}}{T}\right)^4 \sin\left(\pi \frac{T}{T_{0,e}}\right)}{(2a_e)^3 B_C}\right)^{\frac{T_{0,e}}{T}} \times \left(\frac{1}{2k_B T_{0,e} \varepsilon_S \varepsilon_0}\right)^{\frac{T_{0,e}}{T}-1} C_i^{\frac{2T_{0,e}}{T}-1} \quad (2)$$

and the hole current can be expressed as

$$I_{ds,h}(x_0 < x < L) = \frac{W}{L - x_0}\left(\gamma_h \frac{T}{2T_{0,h}} \frac{T}{2T_{0,h} - T}\left(V_d - V_g + V_t\right)^{\frac{2T_{0,h}}{T}}\right) \quad (3)$$

with

$$\gamma_h = \frac{\sigma_{0,h}}{q}\left(\frac{\left(\frac{T_{0,h}}{T}\right)^4 \sin\left(\pi \frac{T}{T_{0,h}}\right)}{(2a_h)^3 B_C}\right)^{\frac{T_{0,h}}{T}} \times \left(\frac{1}{2k_B T_{0,h} \varepsilon_S \varepsilon_0}\right)^{\frac{T_{0,h}}{T}-1} C_i^{\frac{2T_{0,h}}{T}-1} \quad (4)$$

where x is the position in channel parallel to the source drain, x_0 the position in the channel of recombination plane, W and L are the width and channel length of the transistor, respectively, T is the temperature, $T_{0,e}$ and $T_{0,h}$ are the characteristic temperatures that indicate the widths of the exponential DOS for the electrons and holes, respectively, V_t is the threshold voltage,[16,17] q is the elementary charge, k_B is the Boltzmann constant, B_C is a critical number for the onset of percolation (= 2.8 for a 3D amorphous system[17]), C_i is the geometric capacitance of the gate dielectric per unit area (17 nF cm^{-2}), ε_0 is the relative permittivity of a vacuum, ε_s (ca. 3) is the dielectric constant of the semiconductor, $\sigma_{0,e}$ and $\sigma_{0,h}$ are the conductivity pre-factors for the electrons and holes respectively, and finally a_h^{-1} and a_e^{-1} are the wave-function localization length for the holes and electrons, respectively.

From the condition of current conservation ($I_{ds,e}(x < x_0) = I_{ds,h}(x_0 < x)$), the following expression for the position of the recombination zone within the channel, x_0, can be derived

$$x_0 = \frac{\left(V_g - V_t\right)^{\frac{2T_{0,e}}{T}}}{A\left(V_d - V_g + V_t\right)^{\frac{2T_{0,h}}{T}} + \left(V_g - V_t\right)^{\frac{2T_{0,e}}{T}}} \cdot L \quad (5)$$

where

$$A = \frac{\left(2T_{0,e} - T\right)}{\left(2T_{0,h} - T\right)} \frac{T_{0,e}}{T_{0,h}} \frac{\gamma_h}{\gamma_e} \quad (6)$$

Finally, substituting Equation 5 for x_0 into Equation 1 yields:

$$I_{ds} = \frac{W}{L}\left(\gamma_e \frac{T}{2T_{0,e}} \frac{T}{2T_{0,e}-T}(V_g - V_t)^{\frac{2T_{0,e}}{T}} + \gamma_h \frac{T}{2T_{0,h}} \frac{T}{2T_{0,h}-T}(V_d - V_g + V_t)^{\frac{2T_{0,h}}{T}}\right) \quad (7)$$

Using Equation 7 we were able to fit the experimental curves of Figure 2a (symbols) employing two set of parameters, one for the holes and one for the electrons. From the fits, the characteristic temperature of the width of the exponential DOS for both carriers was obtained yielding $T_{0,h} = 585$ K and $T_{0,e} = 514$ K. Furthermore, we obtained $\gamma_h = 2.0 \times 10^{-15}$ and $\gamma_e = 1.0 \times 10^{-14}$. The values of α^{-1} and σ_0 for holes and electrons can be determined from temperature-dependent measurements. However, that is out of the scope of this Communication. V_t, was found to be –2 V for a measurement sweep going from negative to positive gate bias (positive V_d) and 2 V for a sweep going from a positive to a negative gate bias (negative V_d). The observed shift in V_t was attributed to electrical stressing of the device, a well-documented process.[19] The parameter values T_0 and γ obtained for SQ1 are comparable with values reported in the literature for several other organic semiconductors.[16,18] Theoretical curves are represented as the solid lines in Figure 2a. From this figure it is evident that for $V_g - V_t$ biases close to $V_d/2$, a discrepancy between measured and simulated data was observed. We attribute this to parasitic contact effects,[20,21] which were not taken into account in the model. Despite this discrepancy, however, a good description of the experimental data can be obtained in both operating regimes, that is, in hole and electron accumulation.

By substituting the fit parameters into Equation 5 we were able to calculate the position of the recombination zone as a function of V_g at positive V_d voltages. This plot is shown in Figure 3a. As can be seen, the recombination zone could be shifted throughout the channel by tuning the V_g and V_d potential, in agreement with previous experimental observations.[12,13] In order to study the effects of the position of the recombination zone along the channel on I_p/I_{ds}, we have combined the experimental data of Figure 2b with the theoretical predictions of Equation 5. The resulting plot is shown in Figure 3b, where I_p/I_{ds} is plotted versus the calculated position of the recombination zone. From this analysis we found that near the metal contacts a drastic lowering of I_p/I_{ds} occurred. At distances beyond a few hundred nanometers from the contacts, the external efficiency of the device was only weakly dependent on the position of the recombination zone along the channel, if one takes the experimental error (shadowed area) introduced by the dark current in the photodiode current into account. This observation is consistent with the assumption that full recombination takes place in a relatively narrow zone, and provides, thus, further experimental evidence for the validity of the model. From studies performed on organic light-emitting diodes (OLEDs) it is known that the distance

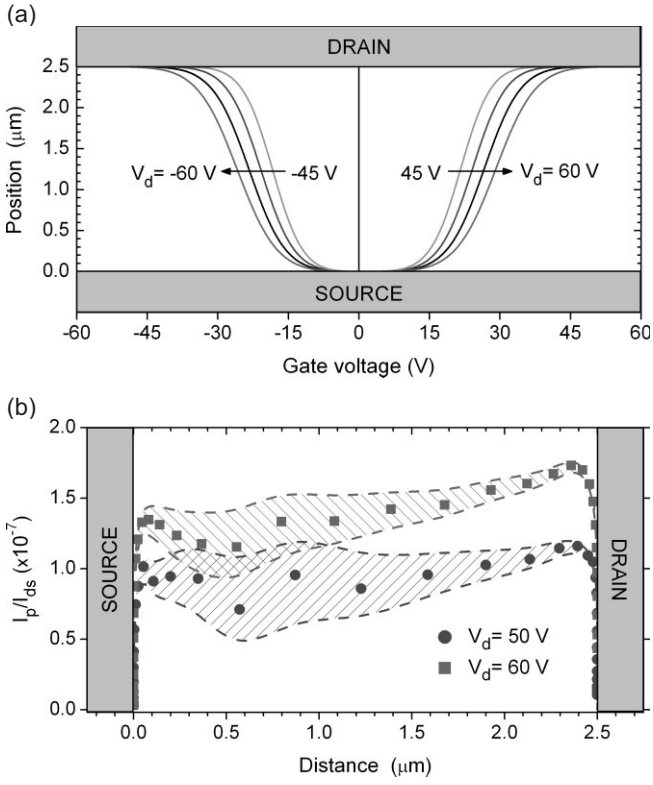

Figure 3. a) The calculated position (source to drain) of the recombination zone (using Eq. 4) versus V_g at different V_d ($\Delta V_d = 5$ V). b) Measured I_p/I_{ds} versus calculated position of the recombination zone at different V_d. Shadowed areas represent the estimated error caused by the photodiodes dark current. The grayed areas represent the position of the source and drain electrodes in space.

of around a hundred nanometers is too large for metal-induced EL quenching to occur.[22] However, a direct comparison between OLEDs and LEOFETs would be inappropriate because of the different device geometry. Another possible explanation for the decay of I_p/I_{ds} near the contacts would be that the recombination zone itself has a width of the order of a hundred nanometers. Such a zone would still be narrow compared to the channel length so that the basic assumption that led to Equation 5 would still remain valid.[16]

In summary, operation of a near-infrared light-emitting ambipolar organic transistor has been demonstrated. The advantage of this device is twofold: i) it employs similar source and drain contacts of gold, and ii) it relies on a single, solution-processable organic semiconductor. Such a device configuration, in combination with the theoretical model presented here, provides a powerful tool towards a better understanding of the various electronic processes within organic materials under different conditions.

Experimental

Device Fabrication: Ambipolar field-effect transistors were fabricated using heavily doped p-type Si wafers as the common gate elec-

ADVANCED MATERIALS

trode with a 200 nm thermally oxidized SiO_2 layer as the gate dielectric. Using conventional photolithography, gold source and drain electrodes were defined in a bottom contact device configuration (Fig. 2a, inset) with channel width (W) and length (L) of 50 cm and 2.5 μm, respectively. A 10 nm layer of Ti was used, acting as an adhesion layer for the Au on SiO_2. The SiO_2 layer was treated with the primer hexamethyldisilazane prior to semiconductor deposition in order to passivate its surface. Films were spun from a 10 mg mL^{-1} solution of SQ1 in chloroform at 800 rpm for half a minute. Freshly prepared devices were annealed in vacuum of 10^{-6} mbar (1 bar = 100 000 Pa) at 115 °C for one hour. All electrical and optical measurements were performed in high vacuum (10^{-6} mbar) at room temperature using an HP 4155C semiconductor parameter analyzer. Light emission was measured using a Si pin-diode (Siemens BPX61) placed in close proximity above the transistors.

Absorption, Electroluminescence, and Photoluminescence Measurements: For UV-vis absorption measurements SQ1 was spin-coated on a glass substrate from a chloroform solution and subsequently annealed at 115 °C. The absorption spectrum was recorded with a Perkin Elmer Labda 950 spectrometer. PL measurements on SQ1 films were performed on the same sample used for the transistor devices fabricated side by side. The film was excited with a 633 nm HeNe laser and the PL spectrum was recorder using a Horiba Jobin Yvon Labram spectrograph equipped with a deep-depletion nitrogen-cooled CCD camera (400–1050 nm). The EL spectrum from the diode structures was measured with an Andor Shamrock SR 303i-A spectrometer equipped with an Andor Idus CCD camera. Cyclic-voltammogram (CV) measurements were performed using a 757 VA Computrace system from Metrohm. The CVs were recorded under an Ar atmosphere in acetonitride/Tetrabutylammoniumhexafluorophosphate on a glassy carbon working electrode. The redox potential was calibrated against the internal reference Fc/Fc^+ couple.

Received: May 8, 2006
Revised: November 6, 2006
Published online: January 25, 2007

[1] G. H. Gelinck, H. E. A. Huitema, E. Van Veenendaal, E. Cantatore, L. Schrijnemakers, J. B. P. H. van der Putten, T. C. T. Geuns, M. Beenhakkers, J. B. Giesbers, B. Huisman, E. J. Meijer, E. Mena Benito, F. J. Touwslager, A. W. Marsman, B. J. E. van Rens, D. M. de Leeuw, *Nat. Mater.* **2004**, *3*, 106.

[2] A. Knobloch, A. Manuelli, A. Bernds, W. Clemens, *J. Appl. Phys.* **2004**, *96*, 2286.

[3] A. Hepp, H. Heil, W. Weise, M. Ahles, R. Schmechel, H. von Seggern, *Phys. Rev. Lett.* **2003**, *91*, 157 406.

[4] C. Santato, R. Capelli, M. A. Loi, M. Murgia, F. Cicoira, V. A. L. Roy, P. Stallinga, R. Zamboni, C. Rost, S. F. Karg, M. Muccini, *Synth. Met.* **2004**, *146*, 329.

[5] T. Oyamada, H. Sasabe, C. Adachi, S. Okuyama, N. Shimoji, K. Matsushige, *Appl. Phys. Lett.* **2005**, *86*, 93 505.

[6] C. Santato, I. Manunza, A. Bonfiglio, F. Cicoira, P. Cosseddu, R. Zamboni, M. Muccini, *Appl. Phys. Lett.* **2005**, *86*, 141 106.

[7] F. Cicoira, C. Santato, M. Melucci, L. Favaretto, M. Gazzano, M. Muccini, G. Barbarella, *Adv. Mater.* **2006**, *18*, 169.

[8] M. Ahles, A. Hepp, R. Schmechel, H. Von Seggern, *Appl. Phys. Lett.* **2004**, *84*, 428.

[9] C. Rost, S. Karg, W. Riess, M. A. Loi, M. Murgia, M. Muccini, *Synth. Met.* **2004**, *146*, 237.

[10] C. Rost, S. Karg, W. Riess, M. A. Loi, M. Murgia, M. Muccini, *Appl. Phys. Lett.* **2004**, *85*, 1613.

[11] J. Reynaert, D. Cheyns, D. Janssen, R. Muller, V. I. Arkhipov, J. Genoe, G. Borghs, P. Heremans, *J. Appl. Phys.* **2005**, *97*, 114 501.

[12] J. Zaumzeil, R. H. Friend, H. Sirringhaus, *Nat. Mater.* **2006**, *5*, 69.

[13] J. S. Swensen, C. Soci, A. J. Heeger, *Appl. Phys. Lett.* **2005**, *87*, 253 511.

[14] M. A. Loi, C. Rost-Bietsch, M. Murgia, S. Karg, W. Riess, M. Muccini, *Adv. Funct. Mater.* **2006**, *16*, 41.

[15] L. Chua, J. Zaumseil, J. Chang, E. C.-W. Ou, P. K.-H. Ho, H. Serringhaus, R. H. Friend, *Nature* **2005**, *434*, 194.

[16] E. C. P. Smits, T. D. Anthopoulos, S. Setayesh, E. van Veenendaal, R. Coehoorn, P. W. M. Blom, B. de Boer, D. M. de Leeuw, *Phys. Rev. B: Condens. Matter* **2006**, *73*, 205 316.

[17] M. C. J. M. Vissenberg, M. Matters, *Phys. Rev. B: Condens. Matter* **1998**, *57*, 12 964.

[18] E. J. Meijer, C. Tanase, P. W. M. Blom, E. van Veenendaal, B.-H. Huisman, D. M. de Leeuw, T. M. Klapwijk, *Appl. Phys. Lett.* **2002**, *80*, 3838.

[19] A. Salleo, R. A. Street, *J. Appl. Phys.* **2003**, *94*, 471.

[20] T. D. Anthopoulos, D. M. de Leeuw, E. Cantatore, S. Setayesh, E. J. Meijer, C. Tanase, J. C. Hummelen, P. W. M. Blom, *Appl. Phys. Lett.* **2004**, *85*, 4205.

[21] T. D. Anthopoulos, C. Tanase, S. Setayesh, E. J. Meijer, J. C. Hummelen, P. W. M. Blom, D. M. Leeuw. *Adv. Mater.* **2004**, *16*, 2174.

[22] a) D. E. Markov, P. W. M. Blom, *Appl. Phys. Lett.* **2005**, *87*, 233 511. b) D. E. Markov, P. W. M. Blom, *Phys. Rev. B: Condens. Matter* **2005**, *72*, 161 401.

